Swiss Federal Institute of Technology, Lausanne

Machine Tool Cooling and Lubrication in the Use Phase

Final Report

Professor: P. Xirouchakis

Assistant: O. I. Avram

Prepared By: M. Adham

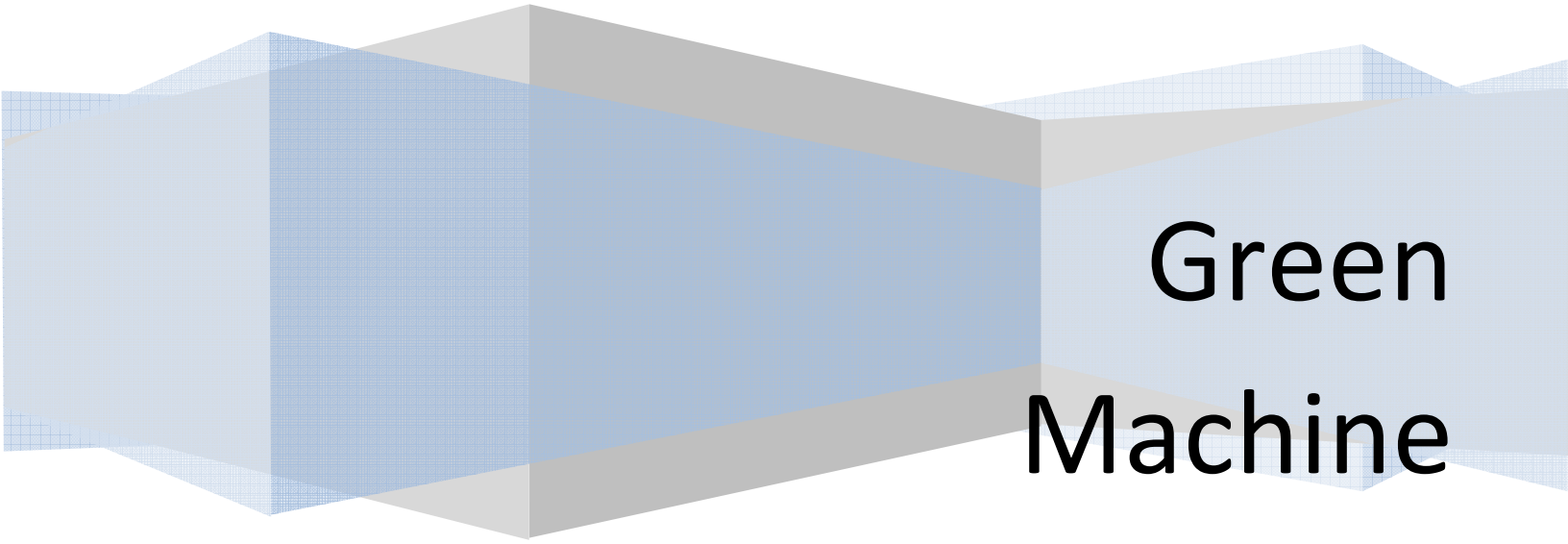

Contents

1.0 Introduction

For machine tool systems, precision is paramount. To obtain the necessary levels of precision and stability in modern systems, the complexity of cooling and lubrication systems has increased. Lubrication and cooling of machine tool systems is vital to reducing friction in contact zones, and to ensure minimal disturbances. Cooling is needed to maintain thermal stability, which results in minimal changes in temperature and thermal expansions. Modern machine tool systems are equipped with various cooling and lubrication subsystems to preserve working conditions and maximize machine life. These subsystems require energy, whether it is in electrical or compressed air form. With the recent advance in green machining practices, a method to quantify the energy consumption of these systems is required, to facilitate means to determine the most energy efficient methods of machining. With the enormous variety of machine tool systems available to industry, it can be difficult to describe models for each subsystem; this report will focus on the two highest energy consuming components: the spindle and the cutting area cooling systems. These sub-systems come in a variety of designs, and this report will outline the most popular systems, and the energy consumption required for each system.

2.0 Sub-System Reference Review

In this report, the cooling and lubrication as a whole is analyzed, and the major power consumption sub-systems are analyzed. The major sources of heat are spindle cooling and lubrication, as well as cutting area cooling/lubrication. There has been significant research done in the areas of heat sources in high speed spindles. This research has been covered in depth by Bossmanns [1], as well as Zhang [2]. These analyses into the heat sources in high speed spindles show that there are two main sources of heat, the heat generated by the motor due to electrical losses, and the heat caused by friction in the bearings of these systems. Bossmanns indicates that when the bearings in these systems are lubricated and cooled using an oil-air mixture, almost all of the heat is transferred to the air due to its high velocity, and that little heat from the bearings will be transferred to the oil, and kept in the spindle structure. In effect in these oil-air systems, the air will act as a bearing coolant. Zhang indicates that there is a significant amount of heat generated by the friction and cutting of the tool on the work piece, and that with short tools, some of this heat can be conducted through the tool into the spindle structure. Zhang also indicates that the amount of heat conducted through the tool will be negligible compared to the amount of heat generated by the spindle drive itself. Bossmanns presents a useful model for determining the heat generation by high speed spindles as a function of frequency, torque and spindle characteristics. Bossmanns also presents a model to determine the heat transfer from the spindle drive to the coolant fluid that evacuates this thermal energy. This heat transfer to the coolant will be evacuated by the spindle's cooling unit.

There are several methods for lubricating the cutting area; oil-air systems, also known as minimum quantity lubrication (MQL) systems, as well as systems that pump a liquid lubricant and apply it directly to the cutting area. There are advantages and shortfalls to each of these systems. Liquid lubricant systems can typically be sub-divided into low and high pressure systems. In low pressure systems, liquid lubricant will typically be applied directly to the cutting surface through an external nozzle. Kovacevic describes three main groups of liquid high pressure lubrication systems: coolant/lubricant jet injected into tool-chip interface through an external nozzle, jet delivered into the clearance between flank and machined surface, and jet injected directly through the tool rake face into tool-chip interface [3]. Kovacevic's results indicate that there is a definite advantage in tool wear as well as heat dissipation when using high pressure systems; the downfall is that these systems employ secondary pumps to achieve these high pressures, which will in turn consume additional power. MQL systems, on the other hand, have become somewhat popular as an alternative means to cutting area lubrication. Attanasio has shown that there are several advantages in using MQL systems for cutting

area lubrication depending on circumstances (materials, speeds, etc), such as reduced cleaning, as well as situations where cooling is undesirable due to thermal shock [4]. Attanasio also shows that MQL lubrication is not a sufficient means of cooling the tool and the workspace, which can be a severe disadvantage in certain cases. In terms of power usage, MQL systems will draw negligible amounts of power from an MTS's power source, as almost all of the work is done by compressed air. While this can be seen as a positive development from a green manufacturing perspective, Yuan has shown that compressed air can be a very inefficient means to provide power [5].

3.0 Spindle Drive Cooling

Figure 1: Example of High-Speed Spindle Layout [6]

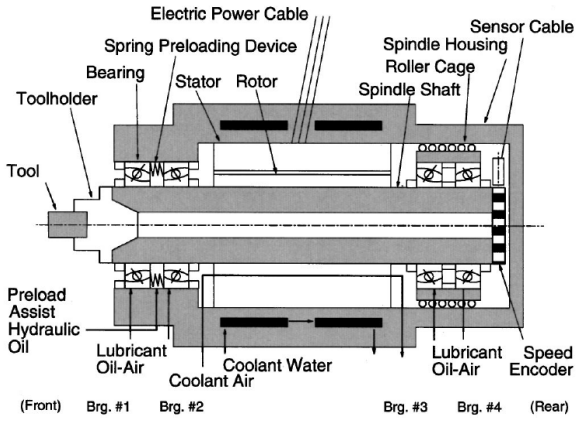

Figure 1 depicts an example of a high-speed motorized spindle architecture (provided by Bossmanss). A motorized spindle, where the spindle motor is built into the spindle, is typically used in High-speed MTS designs, as it removes the need for additional gears and transmissions. The area of interest is the coolant water section. In Figure 1, coolant water will enter the spindle through a rectangular coolant water jacket, circulate around the spindle, and exit the spindle. Bossmanns presents an example of a typical coolant water jacket as shown in Figure 2.

Figure 2: Example of Cooling Water Jacket [7]

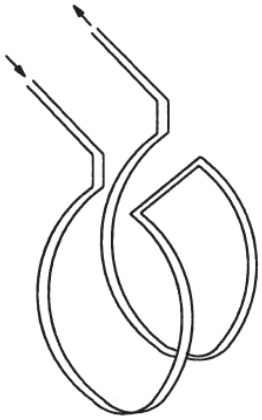

A liquid cooling system for a typical MTS spindle is depicted in Figure 3. Typically, the basic components contained in a spindle cooling system will be the same for motorized spindles, where the motor is contained within the spindle, as well as for spindle systems where the motor is external and corrected through a transmission. The main components of the cooling system are: system to be cooled (spindle), a centrifugal pump for coolant circulation, and an electric flow switch (this may be absent in adjustable frequency drives), and a refrigeration unit. The only components that will draw any significant power are the refrigeration unit, and the centrifugal pump, which will be analysed further.

Figure 3: Sample Spindle Cooling Circuit [8]

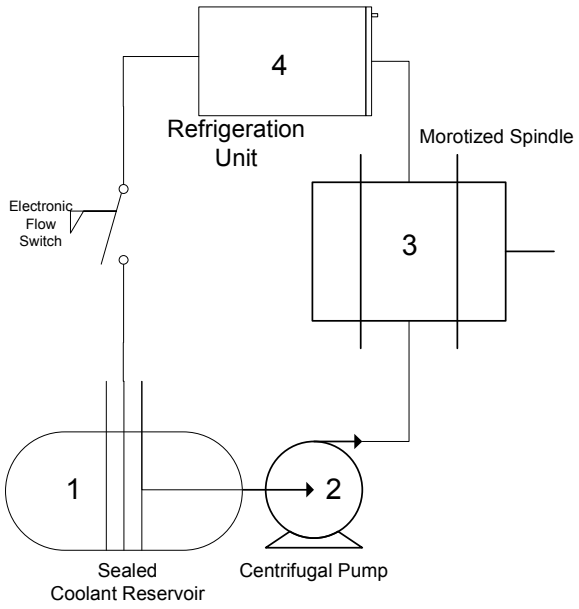

3.1 Coolant Pump

The layout of these features can differ somewhat depending on the MTS, but for each of these systems, the method for calculating overall power will differ based on the extended Bernoulli equation where h_{pump} will be the head supplied by the pump [9]:

$$\frac{p_{in}}{\gamma} + \frac{V_{in}^2}{2g} + z_{in} + h_{pump} = \frac{p_{out}}{\gamma} + \frac{V_{out}^2}{2g} + z_{out} + h_L \quad (1)$$

The subscript "in" refers to the section at the entrance of the pump, while the subscript "out" refers to the entrance to the refrigeration unit (also the output section of the pump). This equation can be simplified for the refrigeration case based on the circuit in Figure 3. To begin, all work is done in between points 2 and 4, in which the pump draws coolant from the reservoir, pumps it through the electro-spindle, and finally into the refrigeration unit. Typically, the refrigeration unit will be placed high above the coolant reservoir, and no work will be needed to circulate the coolant from point 4 to point 1, as this is regulated by the control valve. The parameter p_{in} will be equal to zero (p_{in} , p_{out} are relative pressures with respect to the standard atmospheric pressure), as the coolant is not under pressure at point 2. Similarly, z_{in} and V_{in} will also be equal to zero as the coolant is still upon entering the pump, and it has no potential energy stored as it is at ground level. Therefore the equation can be simplified to:

$$h_{pump} = \frac{V_4^2}{2g} + \frac{p_4}{\gamma} + z_4 + h_L \quad (2)$$

Where V_4 is the velocity of the fluid as it enters the refrigeration unit, which will be proportional to the flow rate: $Q = A \cdot V_4$ (3). p_4 is the pressure of the fluid as it enters the refrigeration unit, and is divided by the specific weight of the fluid. The variable z_4 refers to the vertical distance between point 1 and point 4. Finally, $h_{pump} = \frac{\mathcal{P}}{\gamma Q}$ (4), where $\mathcal{P}$ is the power supplied by the pump, and γ is the specific weight of the liquid [9]. The power supplied by the pump will not directly correlate to the power drawn by the pump, due to the nature of pump efficiency. This efficiency will be determined by the specific pumps efficiency curves, based on flow rate Q, as well as overall head, which will be the sum of $z_4 + h_L$.

One important variable in these equations is h_L , or head loss. This represents the pump head that is lost due to losses in the overall pump system, and will differ heavily depending on the MTS system employed. In general, this term will have to be measured experimentally to obtain an accurate value. In most cases, the head loss of the system can be generalized to contain a number of specific components, and these can be divided into two different components [9], $h_L = h_{L\,major} + h_{L\,minor}$ (5). Major losses can be attributed to a number of factors. The first being the wall shear stress in-between the fluid and the pipe wall. For the purposes of this study, it will be assumed that the flow is wholly turbulent when travelling to and from the spindle structure, as well as while it is passing through the fluid jacket. The head loss due to this

friction can then be calculated using the Darcy-Weisbach equation as follows [9]:

$$h_{L\,friction} = f\frac{l}{D}\frac{V^2}{2g} \quad (6)$$

Where l is the length of pipe through which the coolant is pumped, D the diameter of said pipe, V the velocity of the fluid, and f the friction factor, which can be determined from a Moody chart. Thus, both the Reynolds number, as well as the relative roughness of the pipe is required. As the focus of this report is to develop a general model for energy in the pump system, it will be assumed that the Darcy-Weisbach equation will be sufficient in modeling head loss, and that there are no abnormal friction or turbulent conditions.

Minor losses can be attributed to a number of factors, such as bends in the pipe system, fluid intake design, and filtration. Minor losses will be calculated as [9]:

$$h_{L\,minor} = K_L\frac{V^2}{2g} \quad (7)$$

Where K_L is the loss coefficient. K_L will vary on each aspect of head loss. For example, for square-edged entrance flow, $K_L \cong 0.50$ [9].

The aforementioned models describe a model for calculating the flow of coolant to the spindle cooling channel, but these models cannot always be applied to the energy required to circulate the fluid through the spindle channel itself. Coolant channels differ depending on spindle design. Jang (2008) describes a helical coolant channel for high speed spindles [10]. The flow of the coolant through this channel is fully developed and turbulent. Continuity and momentum equations are presented to model the flow of the coolant through this channel. The method to determine the exact head loss in the cooling channel was outside the scope of this paper, and would most likely have to be determined experimentally. For the purposes of this report, a highly simplified model is used to estimate the head loss of such a system. This report will assume the cooling channel as a presented in Figure 2. In this case, the loss coefficient will simply be that of six 90 degree turns, and four 180 degree curves. This will result in $K_L \cong 1.5$, and $\sum K_L \cong 6 \times 1.5 + 4 \times 1.5 = 15$ [9].

3.2 Heat Generation and Refrigeration

The energy calculations for a refrigeration unit is somewhat more straightforward as in most cases the refrigeration sub-system is a stand alone, packaged, and isolated system. There are several advantages to using packaged units, as it allows the MTS manufacturer to focus on machine design, while not having to design a separate condensing unit. In general, a packaged unit will consist of a condensing unit, and all the necessary components to attach the unit to a machine, as seen in Figure 4.

Figure 4: Sample Pre-Packaged Condensing Unit [11]

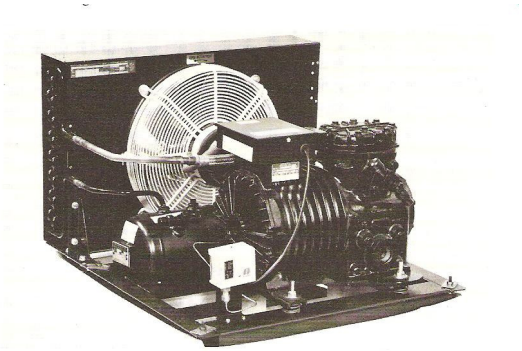

These units will operate on a capacity curve, which is a function of the evaporating temperature (t_{ev}), and the temperature of air into the condenser (t_{atm}). An example of capacity curve is shown in figure 5.

Figure 5: Sample Capacity Curves [11]

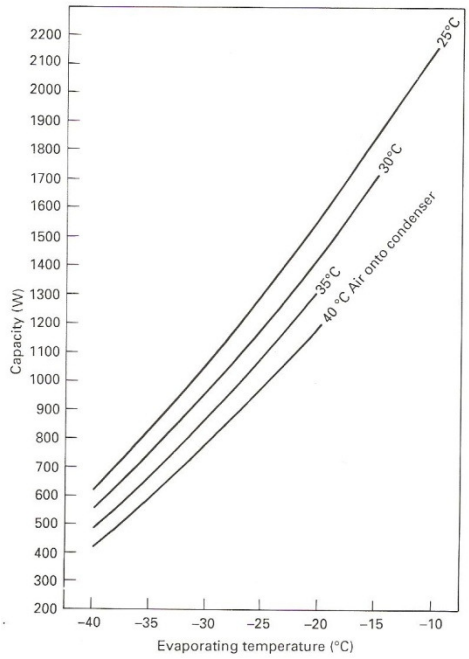

Finally, a packaged unit will operate at an effective efficiency, which is the ratio of how much thermal energy is removed, compared to how much electrical energy is consumed. Therefore the energy use is simply a function of its efficiency, and its energy consumption can be reduced to a function of [12]:

- $\dot{q}_f^+[J]\ thermal\ energy\ removed$
- $\varepsilon_f\ [\%]\ Refrigerator\ efficiency$
- $e_f^+[J]\ Refrigeration\ energy\ consumed$

$$\varepsilon_f = \frac{\dot{q}_f^+}{e_f^+} \quad (8)$$

In general, the refrigeration unit will be set to maintain the coolant at a set temperature, and will consume as much power as necessary to maintain this temperature [11]. We will call this temperature t_{eq}. In this case, the temperature of the coolant over time for the refrigeration unit will resemble Figure 6.

Figure 6: Refrigeration Control System [11]

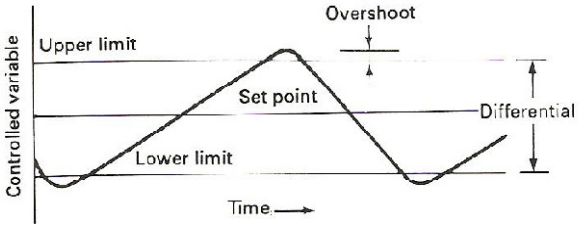

In this chart it is clear that due to the automatic control system present on modern refrigeration units, the temperature of the coolant will be within the upper limit and lower limit of the controlled variable, temperature [11]. This indicates that the refrigeration unit will engage whenever the temperature rises above the upper limit, and disengage whenever the temperature falls below the lower limit. Thus, the power used over time will not be constant, but will spike whenever the unit is engaged. The frequency of this these spikes will depend on the amount of heat transferred to the coolant. If the machine is turned on, but not in use (implying that there is not influx of thermal energy into the condensing unit), it is assumed that this frequency will be constant, as only thermal energy from the atmosphere will be transferred to the coolant. When the machine is engaged, this will not be the case. Also, if the desired temperature t_{eq}, is lower than the ambient temperature of the room, when the machine is initially turned on, higher power will be used to initially cool the liquid, after which the power use will reach an equilibrium. Due to this periodic engagement of the coolant system, it is difficult to determine the exact power the refrigeration unit will consume at any given time. This being the case, a typical refrigeration unit will consume a constant amount of power while engaged, and only be engaged on a down slope of the curve shown in Figure 6. Therefore, the power consumption of the refrigeration unit will resemble Figure 7, where the frequency of the usage is identical to the frequency in Figure 6, and the power will be activated when the temperature passes beyond the upper limit and deactivated when temperature drops below the lower limit.

Figure 7: Refrigeration power consumption

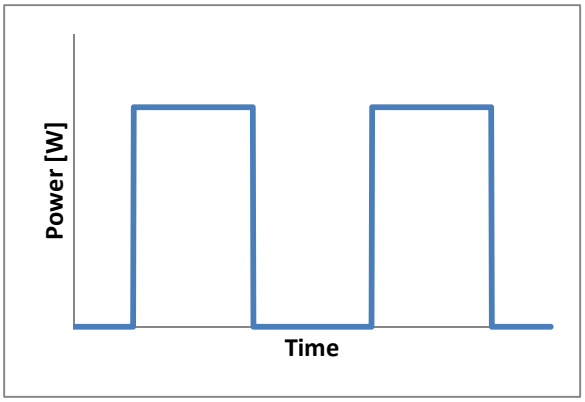

Therefore, the time that the refrigeration unit is activated will depend on the amount of thermal energy transferred to the coolant. It is also possible that this refrigeration unit is used by more than one single cooling sub-system. As a result, any model designed to estimate the power usage of the refrigeration should be designed carefully around the MTS it describes.

A model of calculating the thermal energy generated by the spindle system is required. As mentioned in section 2, Bossmanns hypothesises that the majority of the thermal energy transferred to the coolant will be generated by the spindle motor itself, while the heat generated by the bearings will be transferred to the oil-air mixture [1]. As a part of the analysis, we will now focus on $\dot{Q}^{+}_{motor}[\frac{J}{s}]$, the thermal power generated by the spindle drive. This will be the most significant source of thermal energy that the MTS will deal with. The actual heat generated will differ greatly depending on the electro spindle design, as well as the general motor specifications. As a result exact models for heat generation will be dependent on the specific MTS, but a general model can be described as a function of [13]:

- $\omega_{motor}\ \left[\frac{Rad}{s}\right] angular\ velocity\ of\ spindle$
- $t\ [s]\ time$
- $M_{motor}\ [Nm]\ torque\ on\ motor$
- $\varepsilon_t\ [\%]\ Thermal\ efficiency\ of\ motor$

$$\dot{Q}^{+}_{motor} = \phi(\omega, t, M, \varepsilon_t)$$

As most modern spindle drives are three phase AC induction motors, this report will perform a more in-depth analysis on these types of motors. Bossmanns shows that for a three phase, four pole spindles, the thermal power generated by a spindle drive can be estimated as [1]:

$$\dot{Q}^{+}_{motor} = 2 \times \pi \times f_{motor} \times M_{motor} \times \frac{1-\eta_{motor}}{\eta_{motor}} \quad (9)$$

Where:

- f_{motor}[RPs] speed of motor in revolutions per second
- M_{motor}[Nm] is the motor torque
- $\eta_{motor}$is the actual motor efficiency

This efficiency can be calculated as [1]:

$$\eta_{motor} = \eta_{motor\ max} \times \eta_{spec\ speed} \times \eta_{spec\ load} \quad (10)$$

These are dimensionless parameters which are a function of $\omega_{motor\ rel} = \frac{\omega_{motor}}{\omega_{motor\ max}}$ (11) (angular velocity measured in rad/s) and $load_{motor\ rel} = \frac{M_{motor}}{M_{motor\ max}}$ (12) [1]. The angular velocity of the motor can be calculated as $\omega_{motor} = \frac{N \cdot \pi}{30 \cdot p}$(13), with N being the motor revolutions per minute and p being the number of pole pairs [14]. $\eta_{motor\ max}$ can be determined from tables on general AC motor properties found in typical mechanical engineering handbooks, such as those presented by Avallone in "Marks' Standard Handbook for Mechanical Engineers" [14].

$\eta_{spec\ load}$ can be determined in a table derived by Bossmanns, as seen in Figure 8:

Figure 8: Dimensionless load Efficiency Factor [1]

$load_{m.rel}$	0	.025	.05	.1	.2	.4	.6	.8	1
$\eta_{s.load}$	.01	.28	.6	.7	.83	.93	.97	1	.96

$\eta_{spec\ speed}$ can be determined from experimental data; Bossmanns experimental data was roughly $\eta_{spec\ speed} = .92 + \omega_{motor\ rel} \times .08$ (14).

The torque of the motor will depend on the motor power and revolutions per minute. In general, torque can be calculated to be [14]:

$$M_{motor} = \frac{P_{motor} \cdot 9.550}{N} \quad (15)$$

Where M_{motor} [Nm] is the motor torque, P_{motor} [W] is the motor power and N [RPM] is the motor revolutions per minute. This relationship can be described in as seen in figures 9 and 10, which show the relationship between motor speed, torque and power. These charts show that in general, after the motor reaches its base speed, the torque of the motor will decrease with an increase in speed, while the power will reach a constant value. At values lower than the base speed, the torque will be constant, while power will increase.

Figure 9: Torque of an AC drive over the speed range [15]

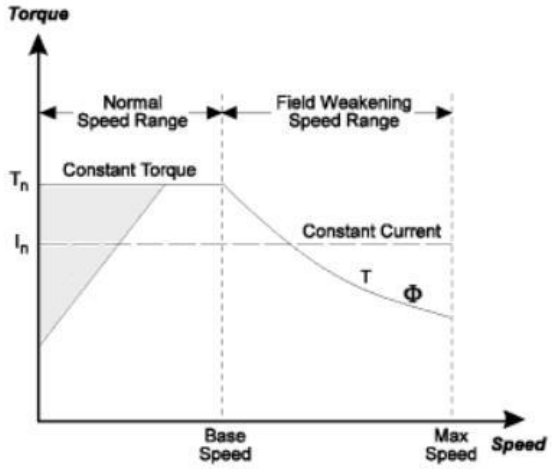

Figure 10: Power of an AC drive over the speed range [15]

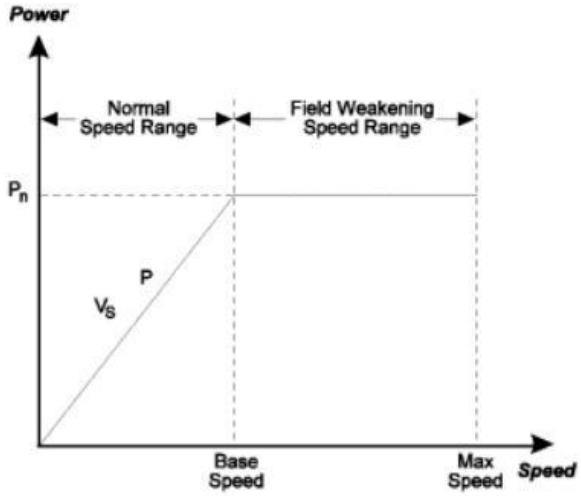

Finally, the heat transfer from the spindle drive to the flowing coolant needs to be considered. Bossmanns hypothesized that this heat transfer is linear, and can be modeled as [1]:

$$\alpha = \frac{0.0225 \cdot \bar{u}^{.3} \cdot \lambda_{fluid}^{.7} \cdot c_p^{3} \cdot \rho_{fluid}^{.3}}{h_{gap}^{.2} \cdot v_{fluid}^{.5}} \quad (16)$$

- α is the heat transfer coefficient
- $\bar{u}$ is the mean velocity of the fluid relative to the solid surface
- v_{fluid} is the kinematic viscosity of the fluid
- h_{gap} is the length of the gap in the fluid channel
- λ_{fluid} is the specific heat capacitance of the fluid
- c_p is the thermal conductivity of the fluid
- ρ_{fluid} is the mass density of the fluid

It should also be noted that the mean velocity of the fluid will depend on the shape of the cooling water jacket. In the case of a rectangular jacket, the mean velocity will equal:

$$\bar{u} = \frac{\dot{v}}{b \cdot h_{gap}} \quad (17)$$

Where $\dot{v}$ is the velocity of the fluid entering the jacket, and $b \cdot h_{gap}$ is the cross sectional area of the jacket.

Now that the amount of heat to be removed is determined, the amount of time that the coolant system must be activated due to the influx of thermal power from the spindle drive can be determined.

$$\dot{Q}^{+}_{motor}\left[\frac{J}{s}\right] \times t_s[s] \times \varepsilon_f \times \frac{1}{E^{+}_{f}}\left[\frac{s}{J}\right] = t_f \quad (18)$$

Where:

- t_s is the time the spindle is activated
- E_f^+ will be the power the refrigeration unit draws when in use
- t_f the additional time the refrigeration unit will have to run to remove the heat generated by the spindle

3.3 Spindle Lubrication

Recently, the use of oil-air systems, also known as MQL (minimum quantity lubrication) has become more popular for lubrication of spindles, linear guides, rack and pinions, as well as the cutting area itself. Certain older systems will more than likely employ an oil circulation system, where oil is circulated through the bearings using a high pressure pump. For these applications, the energy calculation will resemble those of a liquid cooling pump, described in section 3.2. There are certain advantages to these oil air systems, such as higher reliability, as well as less lubricant being used as compared to oil circulation systems, which is a major cost-saving measure [4].

Figure 11: Illustration of Oil-Air Ball Bearing Lubrication System [16]

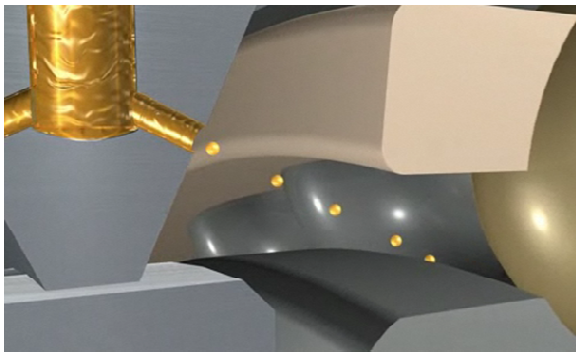

Figure 11 depicts the basis of the oil air system, where ball bearings are lubricated by a minimal amount of lubricant transported through the use of compressed air. When considering the power consumption of such systems, it is important to note that not all power can be measured as electrical potential, as compressed air is now at play. Classically, compressed air has been taken for granted in manufacturing, and its power consumption has not been monitored for specific tasks. This presents a disconnect in minimizing energy consumption, as in certain plants, compressed air efficiency may be at the levels of 60% or less [5]. In terms of the actual work compressed air can perform, the specific power of compressed air can be estimated using the following equation [17]:

$$\dot{E} = Q_m R T_a \left[ln\frac{\dot{P}}{P_a} + \frac{k\left(\frac{T}{T_a} - 1 - ln\frac{T}{T_a}\right)}{k-1} \right] \quad (19)$$

Where:

- k : $Specific\ heat\ Ratio$
- $\dot{E}\ [W]$: $Air\ power$
- $P\ [Pa]$: $Absolute\ air\ pressure$
- $P_a\ [Pa]$: $Air\ pressure\ (atmosphere)$
- $Q_m\ \left[\frac{kg}{s}\right]$: $Air\ mass\ flow\ rate$
- $R\ \left[\frac{J}{kgK}\right]$: $Gas\ Constant$
- $T_a[K]$: $Temperature\ (atmosphere)$
- $T\ [K]$: $Temperature\ (of\ compressed\ air)$

While this equation is useful in determining the power contained in the compressed air, for the purposes of green machines, it is more useful to consider the overall power consumed to create this compressed air, which will vary greatly depending on the air source.

In general, an MQL system will contain the following components:

- Compressed air intake
- Micro pumps
- Oil mixture system

The use of such a system varies somewhat from the cooling pump system. An MQL lubrication system will not run continuously, but will lubricate in bursts, as shown in Figure 11. As a result, to calculate the power used by the lubrication system, the total air consumption of the system is required. The equation will be based on the frequency of micro pump bursts at a given spindle speed, which we will denote as ω_{mql}. We will also define $\dot{A}_{burst}$ as the amount of compressed air consumed in one MQL burst in normal litres. Given these initial values, an overall model to determine the power usage of the lubrication system is:

$$A_{lubrication} = \omega_{mql} \times \dot{A}_{burst} \times q \quad (20)$$

Where:

- q = number of micro pumps
- $\omega_{mql}[\frac{bursts}{minute}]$ varies with spindle design
- $A_{lubrication}$ $[\frac{Nl}{min}]$ overall air consumption of the MQL system

The task is simply to determine the power required to generate a single burst, $A_{lubrication}$. While the actual air power in the burst can be calculated using the equation Kagawa and Cai [17], a more practical model is required for the purposes of this report. In general, a machine manufacturer will report the MQL air consumption of an MTS as a blanket number, in Nl/min (normal litres per minute) or CFM (cubic feet per minute). The power required to generate an air burst will inherently be tied to the power required to generate compressed air, which will typically be independent from the MTS power supply, and provided by an independent air compressor.

The efficiency of these compressors is often confused as a manufacturer will typically provide the efficiency in terms of how much electrical power is required to generate a certain amount of air power (as described in equation 19). These metrics are not useful, and only the capacity and power necessary per unit of compressed air should be considered [18]. The efficiency of the compressor will also depend on usage and capacity. Typically motor drive compressors will present the electrical horsepower input per unit of annual capacity. Therefore care should be taken to cater a model to each specific MTS system, dependent on its environment, whether in large manufacturing plant, or a small machine shop. Figure 12 presents sample data on a two stage motor driven compressor.

Figure 12: Sample Data on Motor Driven Two-Stage compressor [18]

	Full capacity	¾ capacity	½ capacity
Actual Capacity, cubic feet per min	1395	1046	697.5
Bhp at compressor shaft	260	200	143
BHP per 100 CFM actual capacity	18.6	19.25	20.5
Motor efficiency, per cent	92.3	92.3	90.2
HP input per 100 CFM actual capacity	19.95	20.85	22.77

As explained above, the data given presents the electrical hp input per unit as well as the motor efficiency. The two important data points here are "HP input per 100 CFM actual capacity" and "Motor efficiency". Motor efficiency simply indicates the efficiency the motor will reach in generating 1W (or HP) of mechanical power for each 1W (or HP) of electricity drawn. The HP input per CFM capacity indicates how much power is required to generate 100 CFM of compressed air. For a theoretical system that consumes 300Nl/min and is running at a capacity of ¾, using the data above, the actual power use calculations are straightforward:

$$\frac{300\frac{Nl}{Min}}{1} \cdot \frac{1\ cubic\ foot}{28.3\ Nl} = 10.6CFM$$

$$\frac{10.6CFM}{100CFM} \cdot \frac{20.85HP \cdot 745.7W}{1HP} \cdot \frac{1}{.923}$$

$$= 1785.6W$$

These results show that compressed air power usage for such a system is quite high. This equation can be made more accurate by calculating the actual air consumption over time using the equation proposed above, where the power in each air burst is calculated, as opposed to using the manufacturers estimates of air consumption. It should also be noted that the micro pumps used to circulate this air will use a nominal amount of electrical power, but this will be negligible compared to that of the compressed air, as these pumps are more similar to electric flow valves, and use the power of compressed air to do the circulation.

4.0 Cutting area cooling and lubrication

In the area of cutting area cooling and lubrication, there are similarities to the cooling and lubrication of the spindle drive. There are two main methods used for this subsystem: liquid cooling and lubrication, and oil-air MQL cooling and lubrication.

4.1 Cutting area MQL cooling and lubrication

It is becoming more common for MTS to employ an MQL system for cutting area cooling and lubrication. The energy calculations for such systems will be identical to those in section 3.3. While these systems may be advantageous in the amount of lubricant used [4], and overall energy consumed by the MTS, caution should be taken in green machining with these systems, due to the high amount of power required to produce compressed air as calculated above.

4.2 Liquid cooling and lubrication

As in the cooling of spindle drives by means of liquid cooling, the cooling and lubrication of the cutting area is controlled by much of the same components. As in the case of the electro spindle cooling system, the cutting area cooling system is comprised of:

- A pump for liquid circulation
- Electric flow switch

The calculations for pump power are almost identical to those used in section 3.1. As mentioned in section 2, these systems can be divided into both high and low pressure systems. For low pressure systems, there are generally two different pump layouts, pressure throttling and pressure recycling.

Figure 13: Pump/System Characteristic [19]

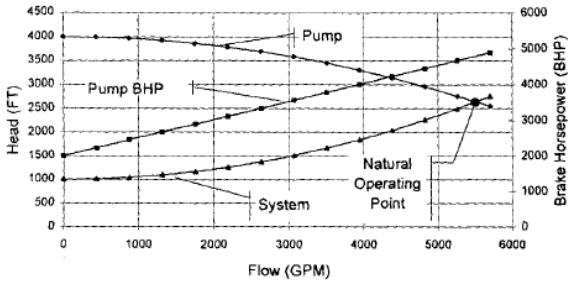

Figure 14: Pressure Throttling System

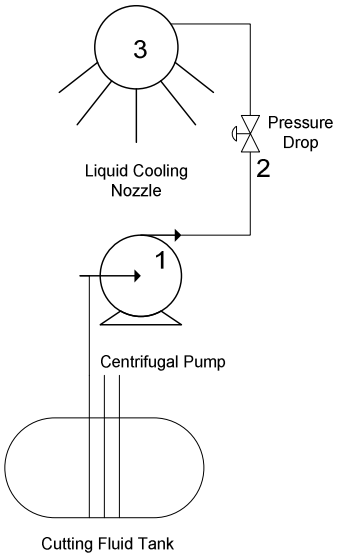

Figure 15: Pressure Recycling System

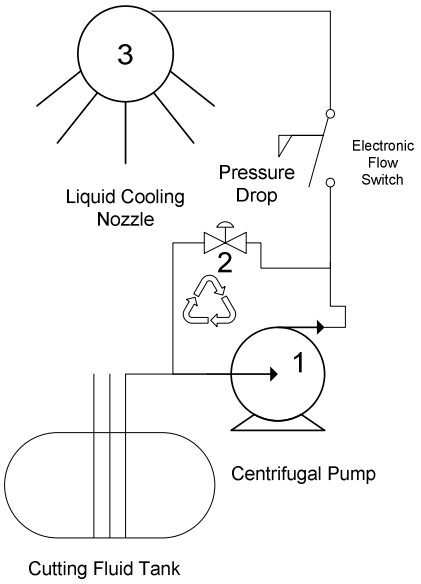

In Figure 14, a pressure throttling system is presented. This is a system where a valve is actively dropping the pressure of the output to ensure the pump is running at its natural operating point, as seen in figure 13. This throttling will consume electrical power from the pump motor as it is actively dropping the pressure and has a flow through it. This is done to ensure the pump is running at its natural operating point [19]. The power calculation for this is quite simple, as in section 3.1.

$$h_{pump} = \frac{p_2}{\gamma} + \frac{V_2^2}{2g} + z_{out} + h_L \quad (21)$$

The major difference in this equation is to note that p_2 will be based on the total head, $z_{out} + h_L$, as well as the flow rate Q. This is to ensure the pump is operating on a curve as seen in Figure 13.

An alternative system is the pressure recycling method, as seen in Figure 15. In these systems, the control valve increases flow through the pump body until it is operating at a discharge that matches its natural curve, requiring the pump to run continuously, which in turn is very inefficient.

$$\frac{p_1}{\gamma} + \frac{V_1^2}{2g} + h_{pump} = \frac{p_2}{\gamma} + \frac{V_2^2}{2g} + z_{out} + h_L \quad (22)$$

One additional important loss factor in MTS can be attributed to high pressure systems, especially those with filtration systems. Certain MTS will be equipped with high pressure systems to improve milling quality, and certain will contain filtration systems for cutting fluids to be delivered through the rake face of the tool [3]. This through-rake face lubrication is achieved through small perforations in the tool. These lubrication systems prove very effective in high speed applications, but require a high degree of filtration due to the low diameter perforations in the tool. These systems also operate at very high pressure. An example of such a system is depicted in Figure 16, as described by Wertheim (1992) [20]. For this reason it can be difficult to determine the exact loss due to the filtration system, but through experimental measurement, the loss of the filtration system can be determined, knowing that $K_L = \phi(geometry, Re)$.

Figure 16: Example High pressure delivery system

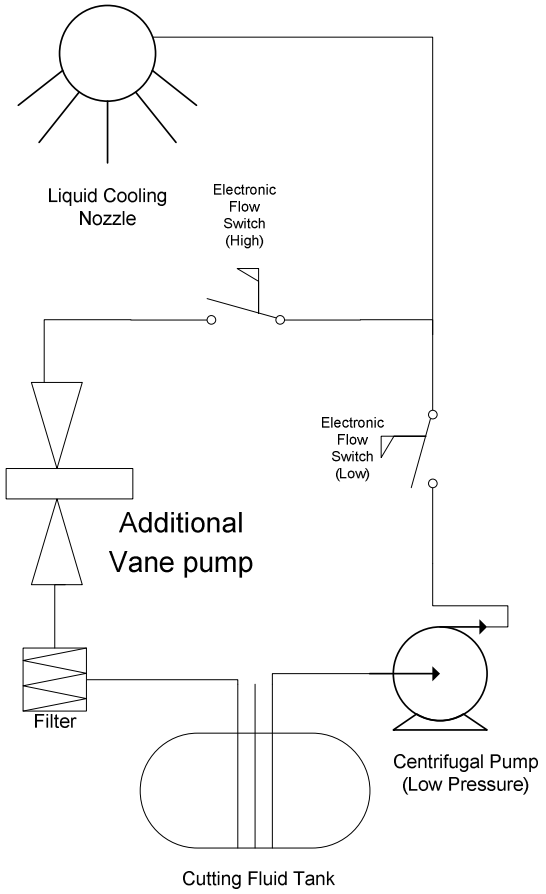

In such a system, the high and low pressure switches are controlled by the machine operator to initiate the high pressure pump and lubrication. In the design presented by Wertheim, the high pressure pump was operating at 16atm, $2l/min$, and pumping through a rake-face hole with a diameter of 3mm. Ignoring all other aspects of head-loss and filtration, simply maintaining this flow rate requires a pump head of:

$$\frac{2l}{min} = \frac{2m^3}{1000}\frac{1}{60s} = \frac{1m^3}{30{,}000s}$$

$$V_{out} = \frac{1m^3}{30{,}000s}\frac{4}{\pi 3^2 \cdot 10^{-6}} = \frac{400}{27\pi} = 4.7m/s$$

$$h_p = \frac{p_{out}}{\gamma} + \frac{V_{out}^2}{2g} = \frac{1621200}{9810} + \frac{4.7^2}{2 * 9.81} = 176m$$

Given that there is no consideration for head-loss in the above equation, this is quite a significant sum to keep the flow maintained.

Generally, cutting area lubrication fluids are not circulated through a cooling unit to remove any of the heat generated by the cutting of the work piece. This cutting does generate a significant amount of heat none the less, and should be considered. While the MTS itself may not always cool the cutting fluid, this heat will have to be dissipated somewhere, whether it be the atmosphere, or through conduction into other machine components. It is therefore useful to look at a model describing the heat generation of the cutting itself. We will call this thermal radiation q_c^+. This thermal radiation can be calculated as follows:

$$q_c^+ = q_f^+ + q_p^+ (23)$$

Where q_f^+ is the thermal radiation from the friction of the tool against the material, and q_p^+ is the thermal radiation created due to the plastic deformation of the material due to the active cutting. Deng and Shet (1999) propose that the temperature rise caused by friction over the time interval Δt can be estimated as [21]:

$$\Delta T_f = \eta_f \frac{\tau \dot{s} \Delta t}{Jc\rho} (24)$$

Where:

- η_f : stands for the portion of frictional work being converted into heat
- τ: shear stress along the frictional interface
- $\dot{s}$: slip velocity
- J: equivalent heat conversion factor
- c: specific heat
- ρ: mass density

The calculation of thermal radiation caused by plastic deformation is not as straightforward. It is proposed that the temperature rise due to plastic deformation can be estimated using the adiabatic heating condition. It is estimated that the local rise in temperature in plastic zones can be calculated as [21]:

$$\Delta T_p = \eta_p \frac{\sigma_e \dot{\varepsilon_p} \Delta t}{Jc\rho} \quad (25)$$

Where:

- η_p : percentage of plastic work transformed into heat
  - Typically $85\% \leq \eta_p \leq 95\%$
- σ_e: the effective stress
- $\dot{\varepsilon_p}$: the effective plastic strain
  - $\dot{\varepsilon_p} = D\left(\frac{\sigma}{\sigma_0} - 1\right)^p$
  - D and p are material parameters [22]
  - σ_0 is the reference stress
- $\dot{s}$: slip velocity
- J: equivalent heat conversion factor
- c: specific heat
- ρ: mass density

More information on the calculation of these parameters can be found in the literature, Deng and Shet (1999). One important factor in this temperature increase is the amount of thermal energy that will be transferred to the cooling fluid, the work piece and the tool. These models have been modeled in certain orthogonal cutting research, but are outside of the scope of this report.

5.0 Sample Calculations

Below are sample calculations for certain cases pertinent to green machining. These calculations are using the assumptions that the motor is that of a C.B. Ferrari motor, with a constant power of 12kW, a maximum torque of 20Nm, a base speed of 5,700RRM, and a maximum speed of 40,000RPM. This information is displayed in figure 17, as provided by the manufacturer.

Figure 17: C.B Ferrari Power vs. RPM curve

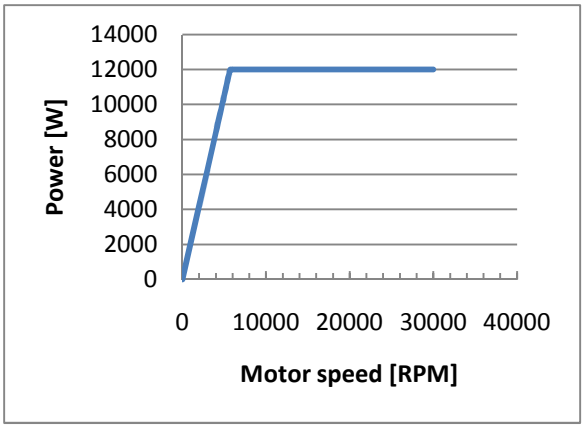

5.1 Thermal Power Generation

As shown in the previous sections, the only power consumption that will vary with spindle speed is the cooling power required to remove thermal output. Through calculations listed in section 3.2, Figure 17 was generated for the sample motor. The values $\eta_{spec\ speed} = .92 + \omega_{motor\ rel} \times .08$ and $\eta_{motor\ max} = .878$ were used [1] [14]. The chart shows that initially, significant heat is generated; this increases rapidly until the motor reaches its base speed of 5,700RPM. After the speed is increased further, the thermal heat generation drops significantly, then takes an upward slope. It should be noted that the odd appearance of the chart is caused by the non-linearity of the constant value $\eta_{spec\ load}$, which is estimated by Bossmanns at certain values, and cannot be easily extrapolated, and as such the value of 7,145W at 1000RPM, which is higher than the power input of 2,100W, and can be rejected due to the nature of torque and power at low speeds, which is not considered by Bossmanns model.

Given that this thermal power will need to be removed by a refrigeration unit, figure 18 was generated to show the amount of time the 1545W refrigeration unit that operates at an efficiency of 85% will have to run to remove this heat. It should be noted that this time is a ratio value, indicating how many seconds the refrigeration unit will have to

run for every second the motor is engaged at that speed.

5.2 Case scenario

Question: In terms of spindle cooling, which is more efficient, cutting at 5,000 RPM(10.5Kw) for 10 seconds, 10,000RPM(1.2kW) for 15 seconds or cutting at 20,000RPM(1.2kW) for 20 seconds?

From calculations in Appendix I, overall, the refrigeration of the spindle will consume $(1545 + 334)W \times 16.25s = 30.53kW \cdot s$ of energy for the 5,000RPM cut compared to $(1545 + 334)W \times 24.76 = 46.52kW \cdot s$ for the 10,000RPM cut, and $(1545 + 334)W \times 37.25s = 69.99kW \cdot s$ for the 20,000RPM cut, indicating that from a refrigeration perspective, the first option of 5,000RPM is most energy efficient.

5.3 Comparison of Power usage of Sub-Systems

Overall, it is interesting to evaluate how the power consumptions of each sub-system compare. For this reason, refrigeration of the spindle, MQL of the cutting area, and high pressure lubrication of the cutting area are compared in figure 20 and 21. The values used are taken from assumptions made throughout this report. The refrigeration unit is that described in the problem in section 5.2. The MQL system is similar to that described in section 3.3 (300 Nl/min). The high pressure cutting area lubrication is similar to that described in section 4.2. It should be noted that the refrigeration proportion is actually significantly higher as it will run even after the spindle is deactivated.

Figure 17: Thermal Power Generated by Motor

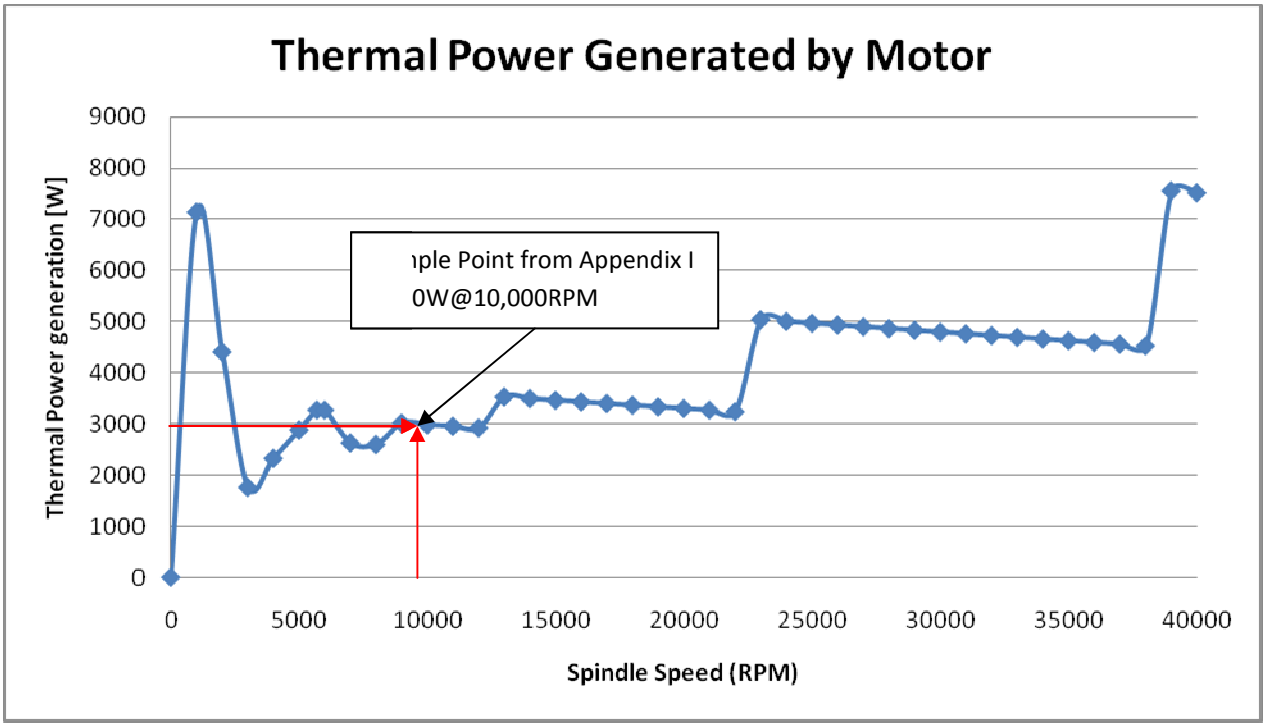

Figure 18: Refrigeration Unit Time

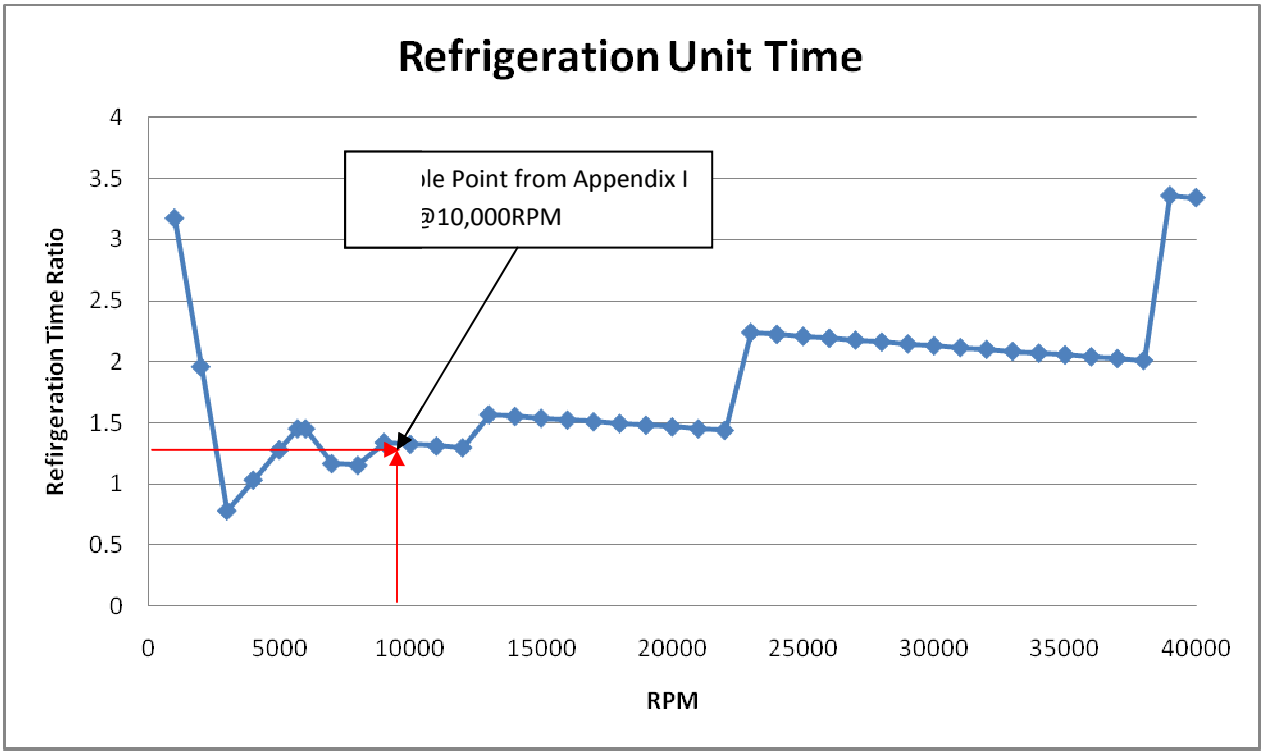

Figure 20: Sub-System power consumption

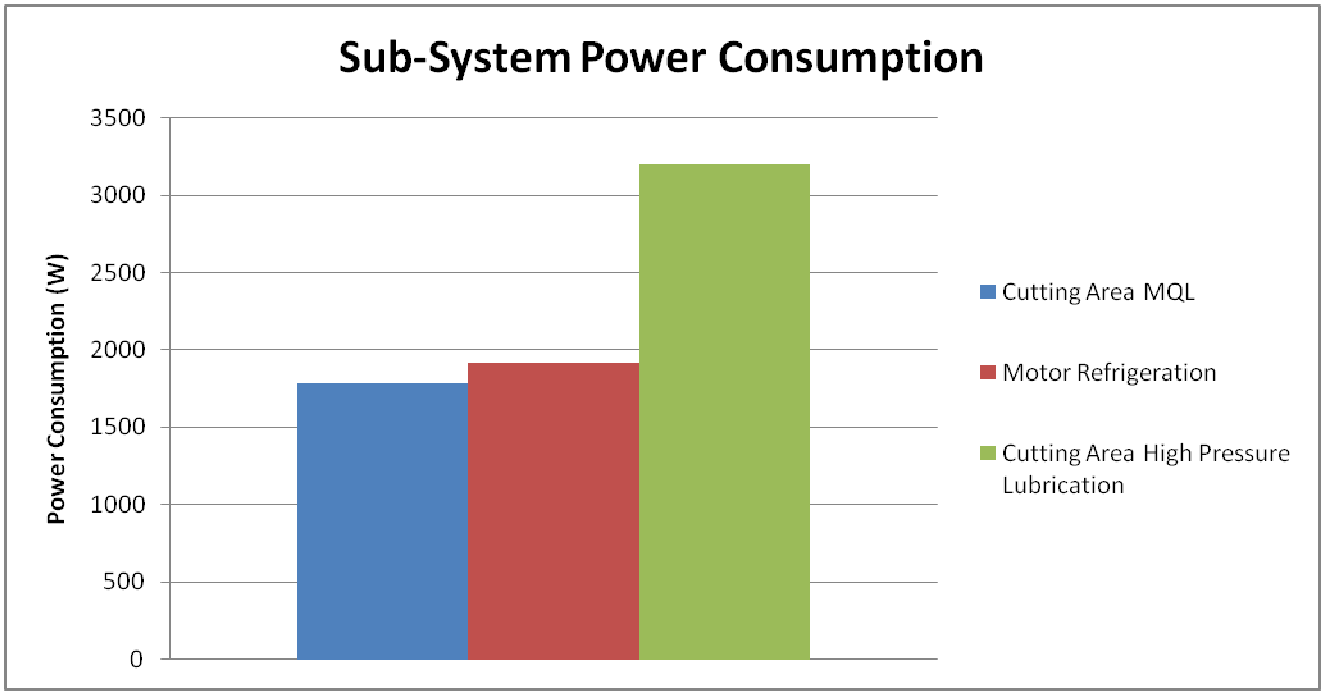

Figure 21: Sub-System power consumption

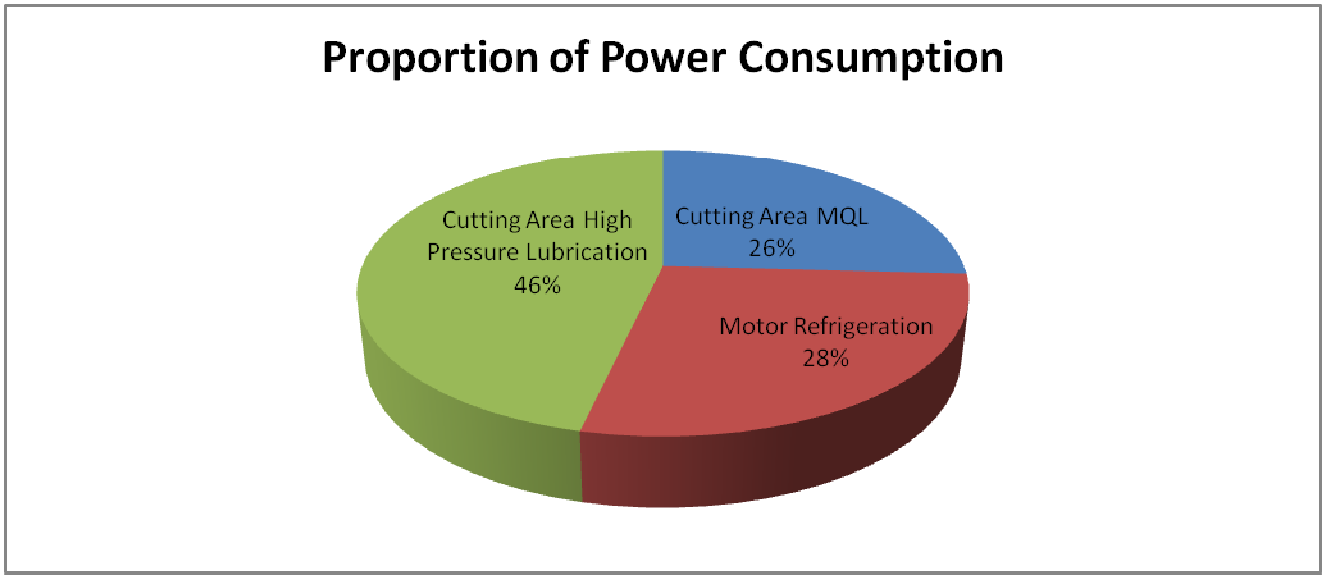

Works Cited

1. **Bossmanns, B.** *Thermo-Mechanical Modeling of Motorized Spindle Systems For High Speed Milling.* West Lafayette : Purdue University, 1997.

2. **Zhang, W.** *High Speed Spindle Heat Sources, therman analysis and bearing protection.* Florida : University of Florida, 1993.

3. *High Pressure Waterjet Cooling/Lubrication To Improve Machining Efficiency In Milling.* **R. Kovacevic, C. Cherukuthotat, M. Mazurkiewicz.** 1995, International Journal of Machine Tools Manufacturing, pp. 1459-1473.

4. *Minimal quantity lubrication in turning: Effect on tool wear.* **A. Attanasio, M. Gelfi, C. Giardini, C. Remino.** 3, s.l. : Wear, 2006, Vol. 260. ISSN 0043-1648.

5. **ChrisY.Yuan, Teresa Zhang, Arvind Rangarajan, David Dornfeld, Bill Ziemba, Rod Whitbeck.** A Decision-Based Analysis of Compressed Air Usage Patterns in Automotive Manufacturing. *Journal of Manufacturing Systems.* 2006, Vol. 25, 4.

6. *A power flow model for high speed motorized spindles - Heat generation Characterization.* **Bossmanns, B., Tu, J. F.** s.l. : Journal of manufacturing science and engineering, 2001, Vol. 123.3, p. 494.

7. *A thermal model for high speed motorized spindles.* **Bossmanns, B., Tu, J. F.** s.l. : International Journal of Machine Tools & Manufacture, 1999, Vol. 39, pp. 1345-1366.

8. **C. B. Ferrari.** Schema Linea RAC Refrigerazione Corpo Elettromandrino. *C.B. Ferrari A152 Instruction Manual.* 2004. 7787523.

9. **Ohiishi, Munson Young.** *Fundamentals of Fluid Mechanics 5th Ed.* s.l. : Wiley, 2006.

10. *3-D numerical and experimental analysis of a built-in motorized high-speed spindle with helical water cooling channel.* **C.H. Chien, J.Y. Jang.** Taiwan : Applied Thermal Engineering, 2008, Vol. 28.

11. **Trott, A. R.** *Refrigeration and Air-Conditioning, 2nd Ed.* s.l. : Butterworth & Co., 1989.

12. **Lucien Borel, Daniel Favrat.** Thermodynamique lineaire des phenomenes irreversibles. *Thermodynamique et Energetique.* Lausanne : Presses Polytechniques et Universitaires Romandes, 2005.

13. **Jufer, Marcel.** Moteurs Synchrones. *Electromecanique.* Lausanne : Presses Polytechniques et Universitaires Romandes, 2004.

14. **E. Avallone, T. Baumeister III.** *Marks' Standard Handbook for Mechanical Engineers 9th Ed.* New York : McGraw-Hill, 1987. pp. 15-46.

15. **Barnes, Malcolm.** *Practical Variable Speed Drives and Power Electronics.* s.l. : Newnes, 2003. ISBN-10: 0750658088.

16. **GMN Paul Müller Industrie GmbH & Co. KG.** GMN 3D animation for GMN high frequency spindles for automatic tool change. [Online] [Cited: March 27, 2009.] http://www.gmn.de/flashplayer/GMN_Spindel_3D_Animation.html.

17. **Maolin Cai, Toshiharu Kagawa.** *Design and Application of Air Power Meter in Compressed Air Systems.* s.l. : IEEE, 2001. pp. 208-212. 0-7695-1266-6/01.

18. **Rollins, John P.** *Compressed Air and Gas Handbook, 5th Ed.* Englewood Cliffs : Prentice Hall, 1989.

19. *The Correct Method Of Calculating Energy Savings To Justify Adjustable Frequency Drives On Pumps.* **Carlson, Ron.** Dhahran : IEEE, 1999. PCIC-99-26.

20. *Influence of high-pressure flushing through the rake face of the cutting tool.* **Wertheim, R.** I, s.l. : CIRP annals ... manufacturing technology, 1992, Vol. 41.

21. *Finite element analysis of the orthogonal metal cutting process.* **Chandrakanth Shet, Xiaomin Deng.**

Opole, Poland : Journal of Materials Processing Technology, 1999, Vol. 105, pp. 95-109.

22. *Finite Element Modeling of Orthogonal Metal Cutting.* **S. A. Erpenbeck, K. Komvopoulos.** Berkeley : Journal of Engineering for Industry, 1991, Vol. 113.

Appendix I: Sample Calculations

For the question posed in section 5.3, the following constants are used:

Coolant Fluid (Water):

- Flow rate $Q = 1\ l/s$
- Density $\rho = 1000\ kg/m^3$
- Diameter of pipe to spindle $D = 4cm$
- Dynamic Viscosity $\mu = 1.003 \times 10^{-3}\ Pa\ s$
- Length of piping $l = 9\ m$
- Gap between spindle and cooling jacket $h_{gap} = 3cm$
- Liquid temperature (controlled) $25 \circ C$
- Coolant jacket width = 5cm
- Roughness of pipes = 0.0015mm
- Number of 90° flanged bends = 6
- Head loss coefficient of cooling jacket = 15
- Head loss coefficient of refrigeration unit = 5
- Height of coolant unit $z_4 = 2\ m$
- Coolant pressure when entering refrigeration unit $p_4 = 3atm$

Motor Characteristics:

- $\eta_{motor\ max}$ = 0.878
- $\eta_{spec\ speed} = .92 + \omega_{spindle\ rel} \times .08$
- $M_{motor\ max}$= 20NM
- $N_{motor\ max}$ = 40,000RPM
- Constant power P = 12,000W

Refrigeration:

- Efficiency ϵ_f=0.85
- Power Usage (without pump)
  - $E_f^+ = 1245W$ when idle
  - $E_f^+ = 1545W$ when engaged
  - Compressor consumes 1245W while the heat exchanger consumes 300W

Pumps:

- Efficiency ϵ=0.85 (will be taken as a constant for sample calculations for simplicity)

Side Notes:

$$1N \triangleq 1\frac{kg\ m}{s^2}$$

$$1J \triangleq 1\frac{kg\ \mathrm{m}^2}{s^2} \triangleq 1\mathrm{Nm}$$

$$1W \triangleq 1J/s$$

$$1\mathrm{l} \triangleq 0.001\mathrm{m}^3$$

$$1\mathrm{atm} \triangleq 101.325\mathrm{kPa}$$

$$1Pa \triangleq 1\frac{\mathrm{N}}{\mathrm{m}^2}$$

$$1\mathrm{g} \triangleq 9{,}81\ \mathrm{m/s}^2$$

$$\gamma \triangleq \rho \cdot g$$

Step 1: Calculate Coolant pump power usage

The coolant pump power usage will be identical for all cases, as the flow rate is constant, and temperature does not affect the power consumption.

- Velocity of fluid V_4 when entering refrigeration unit

$Q = V_4 \times A$ (3)

$$A = \pi \times r^2 = \pi \times 0.02^2 = 0.001257m^2$$

$$V_4 = \frac{1l/s}{0.001257m^2} = \frac{0.001\ m}{0.001257\ s} = 0.8m/s$$

$$\frac{p_4}{\gamma} = \frac{3atm}{1000\frac{kg}{m^3}\cdot g} = \frac{303975Pa}{9810\frac{kg}{m^3}} = 31.00m\ (1)$$

- Head losses

$$h_L = f\frac{l}{D}\frac{V^2}{2g} + \sum K_L\frac{V^2}{2g}\ (5,6,7)$$

$$Re = \frac{\rho VD}{\mu} = \frac{1000\ kg/m^3 \cdot 0.8m/s \cdot 0.04m}{1.003 \times 10^{-3}\ Pa \cdot s} = 31{,}904\ [9]$$

Roughness of pipe $\frac{\varepsilon}{D} = \frac{0.0015mm}{40mm} = 3.75 \cdot 10^{-5}$ [9]

Friction factor $f = 0.015$ from Moody chart in Appendix II.

$$h_{Lmajor} = 0.015 \frac{l}{D} \frac{{V_4}^2}{2g} (6)$$

$$= 0.015 \cdot \frac{9m}{0.04m} \frac{0.8^2}{2 \cdot 9.81} 0.11m$$

$$h_{Lminor} = \sum K_L \frac{V_4^2}{2g} (7)$$

$$\sum K_L = K_{cooling\ jacket} + K_{refrigeration\ unit} + K_{flanged\ bends}$$

$$= 15 + 5 + 6 \times 1.5 = 29$$

$$h_{Lminor} = 29 \cdot \frac{0.8^2}{2 \cdot 9.81} = 0.95m$$

$$h_L = 0.11m + 0.95m = 1.06m$$

$$h_{pump} = \frac{V_4^2}{2g} + \frac{p_4}{\gamma} + z_4 + h_L (2)$$

$$h_{pump} = \frac{0.8^2}{2 \cdot 9.81} + 31.00m + 2m + 1.06m$$

$$= 34.09m$$

$$\mathcal{P} = h_{pump} \times \gamma Q (4)$$

$$= 34.09m \times 1000 \frac{kg}{m^3} \cdot 9.81 \frac{m}{s^2} \cdot 0.001 \frac{m^3}{s} = 334 \frac{J}{s}$$

At an efficiency of 85%, this means the pump will draw: 393W

Step 2: Calculate refrigeration time

First, the motor torque needs to be determined. From the discussion in section 3.2, it is mentioned that the torque will be constant at 20Nm at speeds lower than 5,700RPM. At speeds higher than 5,700RPM, the torque will follow equation (15). From this information, the following chart was generated to display M_{motor} at different speeds.

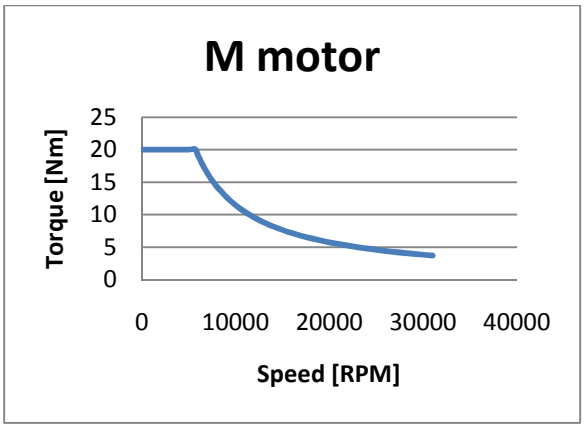

To calculate the difference in time the refrigeration unit will run, first the thermal energy produced by the motor must be calculated. For case 2, *10,000RPM*:

f_{motor} = 10,000RPM/60s = 166.66RPs

For $\omega_{motor\ rel}$, as this is a ratio, there is no need to convert ω_{motor} to rad/s as in equation (13).

$$\omega_{motor\ rel} = \frac{\omega_{motor}}{\omega_{motor\ max}} = \frac{N_{motor}}{N_{motor\ max}} = \frac{10000}{40000}$$

$$= 0.25 (11)$$

$$\eta_{spec\ speed} = .92 + 0.25 \times .08 = 0.94 (14)$$

$$M_{motor} = \frac{9.550 \times 12000}{10000} = 11.46Nm$$ (In constant power range) (15)

$$load_{spindle\ rel} = \frac{M_{motor}}{M_{motor\ max}} = \frac{11.46}{20} = 0.573 (12)$$

From figure 8 , $\eta_{spec\ load} \cong 0.97$

$$\eta_{motor} = 0.878 \times .97 \times .94 = 0.80 (10)$$

$$\dot{Q}^+_{motor} = 2 \times \pi \times f_{motor} \times M_{motor} \times \frac{1 - \eta_{motor}}{\eta_{motor}} (9)$$

$$= 2 \times \pi \times 166.66 \times 11.46 \times \frac{1 - .80}{.80} = 3000W$$

Similarily, for the *5,000RPM* case,

f_{motor} = 5,000/60 = 83.33RPs

$$\omega_{motor\ rel} = \frac{\omega_{motor}}{\omega_{motor\ max}} = \frac{N_{motor}}{N_{motor\ max}} = \frac{5{,}000}{40000} = 0.125$$

$$\eta_{spec\ speed} = .92 + 0.125 \times .08 = 0.93$$

$M_{motor} = 20Nm$ (In constant torque range)

$$load_{motor\ rel} = \frac{M_{motor}}{M_{motor\ max}} = \frac{20}{20} = 1$$

From figure 8 , $\eta_{spec\ load} \cong 0.96$

$$\eta_{motor} = 0.878 \times .96 \times .93 = 0.78$$

$$\dot{Q}^{+}_{motor} = 2 \times \pi \times f_{m\ otor} \times M_{motor} \times \frac{1 - \eta_{motor}}{\eta_{motor}}$$

$$= 2 \times \pi \times 83.33 \times 20 \times \frac{1 - .78}{.78} = 2953W$$

And for the *20,000RPM* case,

f_{motor} = 20,000/60 = 333.33RPs

$$\omega_{motor\ rel} = \frac{\omega_{motor}}{\omega_{motor\ max}} = \frac{N_{motor}}{N_{motor\ max}} = \frac{20{,}000}{40000} = 0.5$$

$$\eta_{spec\ speed} = .92 + 0.5 \times .08 = 0.96$$

$M_{motor} = \frac{9.550 \times 12000}{20000} = 5.73Nm$ (In constant power range)

$$load_{motor\ rel} = \frac{M_{motor}}{M_{motor\ max}} = \frac{5.73}{20} = 0.29$$

From figure 8 , $\eta_{spec\ load} \cong 0.93$

$$\eta_{motor} = 0.878 \times .96 \times .93 = 0.78$$

$$\dot{Q}^{+}_{motor} = 2 \times \pi \times f_{motor} \times M_{motor} \times \frac{1 - \eta_{motor}}{\eta_{motor}}$$

$$= 2 \times \pi \times 333.33 \times 5.73 \times \frac{1 - .78}{.78} = 3385W$$

Therefore, for case 2, the refrigeration unit will have to run for:

$$t_f = 3000 \times 15 \times .85 \times \frac{1}{1545} = 24.76 \text{ (18)}$$

In case 1, the unit will run for

$$t_f = 2953 \times 10 \times .85 \times \frac{1}{1545} = 16.25s \text{ (18)}$$

And in case 3, the unit will run for

$$t_f = 3385 \times 20 \times .85 \times \frac{1}{1545} = 37.25 \text{ (18)}$$

Appendix 2: Moody Chart [9]